Title: Viral delivery of an RNA-guided genome editor for transgene-free plant germline editing

Authors: Trevor Weiss[1], Maris Kamalu[1], Honglue Shi[2,6], Zheng Li[1], Jasmine Amerasekera[1], Benjamin A. Adler[2,3], Michelle Song[1], Kamakshi Vohra[2,11], Gabriel Wirnowski[1], Sidharth Chitkara[1], Charlie Ambrose[1], Noah Steinmetz[1], Ananya Sridharan[1], Diego Sahagun[1], Jillian F. Banfield[2,8,9,10], Jennifer A. Doudna[2,4,6,11,12,13,14], Steven. E. Jacobsen[1,7,15*]

Affiliations:

[1]Department of Molecular, Cell and Developmental Biology, University of California at Los Angeles, Los Angeles, CA 90095, USA

[2]Innovative Genomics Institute, University of California, Berkeley, CA 94720 USA

[3]Department of Bioengineering, University of California, Berkeley, CA 94720 USA

[4]Department of Molecular and Cell Biology, University of California, Berkeley, CA 94720, USA

[5]Department of Biotechnology, Sichuan University, Chengdu, China

[6]Howard Hughes Medical Institute, University of California, Berkeley, CA 94720, USA.

[7]Howard Hughes Medical Institute (HHMI), University of California at Los Angeles, Los Angeles, CA 90095, USA

[8]Department of Earth and Planetary Science, University of California, Berkeley, CA 94720, USA

[9]Department of Environmental Science, Policy and Management, University of California, Berkeley, CA 94720, USA

[10]University of Melbourne, Melbourne, Australia

[11]California Institute for Quantitative Biosciences (QB3), University of California, Berkeley, CA 94720, USA

[12]Department of Chemistry, University of California, Berkeley, CA 94720, USA

[13]MBIB Division, Lawrence Berkeley National Laboratory, Berkeley, CA 94720, USA

[14]Gladstone Institutes, University of California, San Francisco, CA 94158, USA

[15]Lead contact

*Corresponding author. Email: jacobsen@ucla.edu

Abstract: Genome editing is transforming plant biology by enabling precise DNA modifications. However, delivery of editing systems into plants remains challenging, often requiring slow, genotype-specific methods such as tissue culture or transformation. Plant viruses, which naturally infect and spread to most tissues, present a promising delivery system for editing reagents. But most viruses have limited cargo capacities, restricting their ability to carry large CRISPR-Cas systems. Here, we engineered tobacco rattle virus to carry the compact RNA-guided TnpB enzyme ISYmu1 and its guide RNA. This innovation allowed transgene-free editing of *Arabidopsis thaliana* in a single step, with edits inherited in the subsequent generation. By overcoming traditional reagent delivery barriers, this approach offers a novel platform for genome editing, which can greatly accelerate plant biotechnology and basic research.

Main Text:

Programmable RNA-guided endonucleases including CRISPR-Cas9 are driving advances in genome editing for both fundamental research and biotechnology. The ability to genetically modify plant genomes has allowed for the creation of rationally designed phenotypes. However, efficient delivery of genome editing reagents to plants remains a major challenge. The most common strategy is to encode RNA-guided genome editors (e.g. CRISPR-Cas enzymes) within transgenes and use tissue culture and plant transformation approaches to make transgenic plants, after which genetic crosses are required to remove the transgenic material but retain the edits (*1–3*). However, current plant transformation methods are limited to specific species and genotypes, require considerable time, resources and technical expertise, and can cause unintended changes to the genome and epigenome (*1*).

One approach to circumvent these limitations is to use plant viral vectors to deliver genome editing reagents. For example, several viral vectors have been engineered to encode guide RNAs (gRNAs) for delivery to transgenic plants already expressing Cas9, resulting in somatic and germline editing and transmission of edits to the next generation (*4–7*). Because plants have evolved mechanisms to restrict viral infection of meristems and germ cells, most viruses are rarely sexually transmitted (*8*). However, transient invasion of meristem cells by viral RNAs encoding gRNAs allows these cells to be edited, and for these edits to be seed transmissible (*4–7*). While these approaches represent meaningful advances, they still require the use of transgenic plants. Encoding entire CRISPR-Cas systems within RNA viral vectors would eliminate the need for transgenic plants, but has not been possible due to the limited cargo capacity of most plant viruses (*4–7, 9*).

To overcome this stringent cargo size limit, we explored the potential of TnpB, a class of ultracompact RNA-guided endonucleases (~400 amino acids) (*10–12*), to be encoded in a plant RNA viral vector. As ancestors of Cas enzymes, TnpBs similarly utilize a programmable RNA guide, called an omega RNA (ωRNA), to be directed to any target site and induce genome edits. Leveraging its compact size, we demonstrate a rapid, one-step, transgene-free germline editing method in *Arabidopsis* by encoding ISYmu1 TnpB (382 amino acids) (*13*) and it's guide RNA in a single transcript within the tobacco rattle virus (TRV).

Optimization of TnpBs for plant genome editing

Previously, TnpBs ISDra2, ISYmu1 and ISAam1 were shown to be capable of targeted genome editing in mammalian cells, and ISDra2 and ISYmu1 in monocot rice plant cells (*10, 13–15*). Here, we tested the ISDra2, ISYmu1 and ISAam1 TnpBs for genome editing in the dicot plant, *Arabidopsis*. Given the single cargo site in the TRV vector that is typically used, we sought to express both the TnpB protein and its guide RNA within the same mRNA transcript under a single promoter, similar to their natural expression arrangement (*10–12*).

To test the activities of TnpB and its gRNA encoded in a single transcript, we first expressed these three TnpBs and assessed their RNA-guided plasmid interference activities in bacteria. We co-expressed the TnpB and gRNA from the same promoter as a single mRNA transcript, maintaining their natural sequences without codon optimization. We compared two configurations of the 3'-guide region: one extended continuously without a terminator to mimic the natural TnpB condition, and another capped by the hepatitis delta virus (HDV) ribozyme, as previously used in bacteria (*10*) (fig. S1). Our results showed that without the HDV ribozyme, only ISDra2 demonstrated plasmid interference activity whereas with the HDV ribozyme, all three TnpBs exhibited robust activity at both 26°C and 37°C (Fig. 1A, S2). These findings revealed that single transcript expression cassettes with an HDV ribozyme sequence at the 3' end are capable of cleaving plasmid DNA in bacteria.

To test the single expression cassette for targeted genome editing in *Arabidopsis*, we used the *AtUBQ10* promoter to drive expression of the TnpB and a gRNA targeting the PHYTOENE DESATURASE3 (*AtPDS3*) gene region, followed by the HDV ribozyme and rbcS-E9 terminator (Fig. 1B). We tested twenty ISDra2 sites, ten ISYmu1 sites, and seven ISAam1 sites for editing capabilities in *Arabidopsis* protoplast cells (table S1) (*16*). ISDra2 and ISYmu1 demonstrated active editing ranging from 0-4.8% and 0.1-4.2%, respectively, as measured by next generation amplicon sequencing (amp-seq). ISAam1 was much less active, ranging from 0-0.3% editing efficiency (fig. S3A). On average, we observed editing efficiencies of 1% for ISDra2, 2.1% for ISYmu1 and 0.1% for ISAam1 (Fig. 1C). In line with previous reports, the DNA repair profiles consisted of deletion-dominant repair outcomes for all three TnpBs (fig. S3B) (*10, 13, 14*). These data demonstrate that ISDra2, ISYmu1 and ISAam1 are all capable of targeted genome editing in *Arabidopsis* plant cells using the single transcript expression design.

To evaluate TnpB-mediated editing in transgenic plants we selected ISYmu1, as it demonstrated the highest average editing efficiency in *Arabidopsis* protoplast cells and was shown to exhibit no off-target editing in plants (*14*). Two gRNAs with the most active editing were selected, each targeting a unique genomic context. gRNA2 targeted the coding region of *AtPDS3* whereas gRNA12 targeted the promoter region directly upstream of the *AtPDS3* gene. Transgenic plants were created via standard floral dip transformation utilizing the same plasmids as for the protoplast experiments (*17*). To test for sensitivity to temperature, transgenic plants expressing ISYmu1 were either grown at room temperature or subjected to a heat shock treatment. We tested editing in wild type (WT) plants, as well as in the *rna dependent rna polymerase 6* (*rdr6*) mutant which is known to reduce transgene silencing (*18*). Analysis using amp-seq revealed an average editing efficiency of 1.6% and 2.5% for gRNA2 in WT and *rdr6*, respectively (Fig. 1D). Analysis of gRNA12 revealed greater editing than gRNA2, averaging 44.9% editing in WT and 75.5% in *rdr6* (Fig. 1E). Comparison of editing efficiency in the plants grown at room temperature with those that received the heat shock treatment revealed a preference for increased temperature for both target sites in the WT background, demonstrating 6.3-fold and 1.4-fold increases in editing for gRNA2 and gRNA12, respectively (Fig. 1D, E). In *rdr6* we observed a 13-fold increase in editing for gRNA2, but little change in editing for gRNA12 (Fig. 1D, E). These data demonstrate that ISYmu1, encoded as a transgene, is capable of performing efficient genome editing in *Arabidopsis* plants, and that heat treatment and the *rdr6* silencing mutant can be used to increase editing efficiency.

TRV-mediated somatic genome editing by ISYmu1

TRV is a bipartite RNA virus composed of TRV1 and TRV2 (Fig. 2A). Previous work has shown that the TRV2 RNA can be engineered by inserting a cargo expression cassette

136 downstream of the pea early browning virus promoter (pPEBV) (Fig. 2A) (*19, 20*). To test
137 ISYmu1 for genome editing capabilities via TRV delivery to *Arabidopsis*, we engineered two
138 TRV2 Cargo Architectures. In TRV2 Architecture_A, the $tRNA^{Ileu}$ was directly downstream of
139 the TnpB and gRNA sequences (Fig. 2A). In TRV2 Architecture_B, we placed an HDV
140 ribozyme sequence between the guide and $tRNA^{Ileu}$ sequences to assist in 3' guide RNA
141 processing (Fig. 2A). We included $tRNA^{Ileu}$ in both designs as it was shown to promote systemic
142 TRV movement and invasion of meristem cells (*19, 20*).
143 We evaluated TRV-mediated editing potential with gRNA2 using both TRV2
144 Architecture_A and Architecture_B. gRNA2 was selected because it targets the *AtPDS3* coding
145 sequence, enabling easy phenotypic screening for editing due to white photobleaching of cells
146 containing biallelic mutations (*19, 20*). We delivered TRV vectors to both WT and the *ku70*
147 genetic mutant. *Ku70* plays a role in the nonhomologous end joining (NHEJ) double strand break
148 (DSB) repair pathway (*21*). ISYmu1-mediated editing efficiency should be greater in the *ku70*
149 genotype if double stranded breaks generated by ISYmu1 are repaired through NHEJ. Each
150 TRV2 plasmid was co-delivered with the TRV1 plasmid to *Arabidopsis* plants using the
151 agroflood method (*20*). White speckles were observed on some of the leaves around three weeks
152 post agroflooding, indicating sectors of cells containing biallelic mutations in the target *AtPDS3*
153 gene (Fig. 2B). Amp-seq analysis revealed an average of 0.1% and 0% editing efficiency in leaf
154 tissue of WT and *ku70* plants agroflooded with TRV2 Architecture_A and grown under room
155 temperature, respectively (Fig. 2C). For the heat shock treated plants, we observed an average
156 editing efficiency of 0.4% in WT and 0.7% in *ku70* plants agroflooded with TRV2
157 Architecture_A (Fig. 2C). Using TRV2 Architecture_B we observed an average 0.6% and 2%
158 editing in WT and *ku70*, respectively, for the room temperature grown plants. For the plants that
159 received TRV Architecture_B and a heat shock, we observed an average editing efficiency of
160 3.3% in WT and 8.9% in *ku70* (Fig. 2C). These results show that Architecture_B, containing the
161 HDV ribozyme, generated higher editing than Architecture_A, and that the *ku70* mutant can
162 enhance ISYmu1 editing efficiency. Analysis of the repair outcomes in WT indicated a deletion-
163 dominant profile, consistent with our protoplast experiment (Fig. 2D).
164 Next, we tested gRNA12 utilizing the TRV2 Architecture_B, since this architecture
165 demonstrated the highest levels of activity for gRNA2. Using the same agroflood approach
166 described above, we observed an average 8.51% and 4.27% editing efficiency in room
167 temperature and heat treatment growth conditions, respectively (Fig. 2E). Further, 6/57 plants
168 displayed editing greater than 40%, with four greater than 75%, when the room temperature
169 treatment was used (Fig. 2E). Analysis of the repair outcomes again showed a deletion dominant
170 profile (Fig. 2F).
171
172 **TRV-mediated germline genome editing with ISYmu1**
173 To test for heritability of edited alleles in the next generation, seeds were collected from a
174 WT plant showing 54.54% somatic editing using the TRV2 Architecture_B design with gRNA2
175 that underwent heat shock treatment. In total, 2318 seeds were sown on ½ MS plates containing
176 3% sucrose. After ten days, 68 albino seedlings were observed, suggesting biallelic mutations in
177 the *AtPDS3* gene (Fig. 3A). To confirm *AtPDS3* was mutated we performed Sanger sequencing
178 on the two white seedlings shown in Fig. 3A, which revealed both plants to be homozygous for a
179 4 bp frame-shift deletion (Fig. 3B). To further characterize transmission of edited alleles, amp-
180 seq on 209 seedlings (41 albino and 168 green) showed that all of the albino seedlings contained
181 biallelic mutations, with the majority of mutations being the 4 bp deletion observed in Fig. 3B
182 (table S2). Of the 168 green seedlings, eight were heterozygous (4bp deletion/WT) (table S2). It
183 has been demonstrated that TRV is not sexually transmitted to the progeny of an infected parent

plant (*19, 20*). To confirm the absence of TRV in the progeny, RT-Polymerase Chain Reaction (PCR) was performed on six albino plants harboring homozygous 4 bp deletions at *AtPDS3*. Consistent with the literature, TRV was not detected in any of the albino plants (fig. S4) (*19, 20*). These data indicate that TRV-mediated biallelic gene edits using ISYmu1 are heritable and virus-free.

Conclusion

A long-term goal of plant scientists has been the development of fast and easy means of editing plant genomes without the need for tissue culture and transgenesis. Here, we developed an approach utilizing the ultracompact site-specific TnpB genome editor, ISYmu1, together with tobacco rattle virus, for heritable plant genome editing. These results should accelerate high throughput genome editing for both basic and applied research. We anticipate this approach will be applicable to other novel TnpBs, different viral vectors and other plant species for genome editing. Recent work has uncovered many TnpB systems from diverse microbial sources, including enzymes with unique PAM sequence specificities (*22*), which can increase the range of target DNA sequences that could be edited using this approach. The TRV virus used in this study has a broad host range of over 400 species, including many solanaceous plants such as tomato, ornamental plants, and crops (*23*). Additionally, plant viruses with similar cargo capacities such as Potato Virus X and Barley Stripe Mosaic Virus are likely to be amenable to this approach since it has been demonstrated they are capable of viral-mediated heritable gene editing by delivering the gRNA to a Cas9-expressing transgenic plant (*24*). In addition to being an important tool for crop biotechnology, viral delivery of TnpBs could enable high throughput CRISPR screens in model plant species such as *Arabidopsis*, further unlocking their potential for genetic discovery.

References and Notes

1. F. Altpeter, N. M. Springer, L. E. Bartley, A. E. Blechl, T. P. Brutnell, V. Citovsky, L. J. Conrad, S. B. Gelvin, D. P. Jackson, A. P. Kausch, P. G. Lemaux, J. I. Medford, M. L. Orozco-Cárdenas, D. M. Tricoli, J. Van Eck, D. F. Voytas, V. Walbot, K. Wang, Z. J. Zhang, C. N. Stewart Jr, Advancing Crop Transformation in the Era of Genome Editing. *Plant Cell* **28**, 1510–1520 (2016).

2. K. Chen, Y. Wang, R. Zhang, H. Zhang, C. Gao, CRISPR/Cas Genome Editing and Precision Plant Breeding in Agriculture. *Annu. Rev. Plant Biol.* **70**, 667–697 (2019).

3. R. A. Nasti, D. F. Voytas, Attaining the promise of plant gene editing at scale. *Proceedings of the National Academy of Sciences* **118**, e2004846117 (2021).

4. Z. Ali, A. Abul-faraj, L. Li, N. Ghosh, M. Piatek, A. Mahjoub, M. Aouida, A. Piatek, N. J. Baltes, D. F. Voytas, S. Dinesh-Kumar, M. M. Mahfouz, Efficient Virus-Mediated Genome Editing in Plants Using the CRISPR/Cas9 System. *Mol. Plant* **8**, 1288–1291 (2015).

5. E. E. Ellison, J. C. Chamness, D. F. Voytas, Viruses as vectors for the delivery of gene-editing reagents. (2021).

224 6. B. M. Beernink, R. R. Lappe, M. Bredow, S. A. Whitham, Impacts of RNA Mobility Signals on
225 Virus Induced Somatic and Germline Gene Editing. *Front Genome Ed* **4**, 925088 (2022).

226 7. M. Uranga, V. Aragonés, S. Selma, M. Vázquez-Vilar, D. Orzáez, J.-A. Daròs, Efficient Cas9
227 multiplex editing using unspaced sgRNA arrays engineering in a Potato virus X vector. *Plant J.*
228 **106**, 555–565 (2021).

229 8. G. Bradamante, O. Mittelsten Scheid, M. Incarbone, Under siege: virus control in plant
230 meristems and progeny. *Plant Cell* **33**, 2523–2537 (2021).

231 9. B. Ghoshal, B. Vong, C. L. Picard, S. Feng, J. M. Tam, S. E. Jacobsen, A viral guide RNA
232 delivery system for CRISPR-based transcriptional activation and heritable targeted DNA
233 demethylation in Arabidopsis thaliana. *PLoS Genet.* **16**, e1008983 (2020).

234 10. T. Karvelis, G. Druteika, G. Bigelyte, K. Budre, R. Zedaveinyte, A. Silanskas, D. Kazlauskas, Č.
235 Venclovas, V. Siksnys, Transposon-associated TnpB is a programmable RNA-guided DNA
236 endonuclease. *Nature* **599**, 692–696 (2021).

237 11. H. Altae-Tran, S. Kannan, F. E. Demircioglu, R. Oshiro, S. P. Nety, L. J. McKay, M. Dlakić, W.
238 P. Inskeep, K. S. Makarova, R. K. Macrae, E. V. Koonin, F. Zhang, The widespread IS200/IS605
239 transposon family encodes diverse programmable RNA-guided endonucleases. *Science* **374**, 57–
240 65 (2021).

241 12. C. Meers, H. C. Le, S. R. Pesari, F. T. Hoffmann, M. W. G. Walker, J. Gezelle, S. Tang, S. H.
242 Sternberg, Transposon-encoded nucleases use guide RNAs to promote their selfish spread.
243 *Nature* **622**, 863–871 (2023).

244 13. G. Xiang, Y. Li, J. Sun, Y. Huo, S. Cao, Y. Cao, Y. Guo, L. Yang, Y. Cai, Y. E. Zhang, H.
245 Wang, Evolutionary mining and functional characterization of TnpB nucleases identify efficient
246 miniature genome editors. *Nat. Biotechnol.*, 1–13 (2023).

247 14. Q. Li, Y. Wang, Z. Hou, H. Zong, X. Wang, Y. E. Zhang, H. Wang, H. Chen, W. Wang, K.
248 Duan, Genome editing in plants using the TnpB transposase system. *aBIOTECH*, doi:
249 10.1007/s42994-024-00172-6 (2024).

250 15. Z. Li, R. Guo, X. Sun, G. Li, Z. Shao, X. Huo, R. Yang, X. Liu, X. Cao, H. Zhang, W. Zhang, X.
251 Zhang, S. Ma, M. Zhang, Y. Liu, Y. Yao, J. Shi, H. Yang, C. Hu, Y. Zhou, C. Xu, Engineering a
252 transposon-associated TnpB-ωRNA system for efficient gene editing and phenotypic correction
253 of a tyrosinaemia mouse model. *Nat. Commun.* **15**, 1–11 (2024).

254 16. S.-D. Yoo, Y.-H. Cho, J. Sheen, Arabidopsis mesophyll protoplasts: a versatile cell system for
255 transient gene expression analysis. *Nat. Protoc.* **2**, 1565–1572 (2007).

256 17. X. Zhang, R. Henriques, S.-S. Lin, Q.-W. Niu, N.-H. Chua, Agrobacterium-mediated
257 transformation of Arabidopsis thaliana using the floral dip method. *Nat. Protoc.* **1**, 641–646
258 (2006).

259 18. M. Wang, Z. Zhong, J. Gallego-Bartolomé, Z. Li, S. Feng, H. Y. Kuo, R. L. Kan, H. Lam, J. C.
260 Richey, L. Tang, J. Zhou, M. Liu, Y. Jami-Alahmadi, J. Wohlschlegel, S. E. Jacobsen, A gene

261 silencing screen uncovers diverse tools for targeted gene repression in Arabidopsis. *Nature*
262 *Plants* **9**, 460–472 (2023).

263 19. E. E. Ellison, U. Nagalakshmi, M. E. Gamo, P.-J. Huang, S. Dinesh-Kumar, D. F. Voytas,
264 Multiplexed heritable gene editing using RNA viruses and mobile single guide RNAs. *Nat Plants*
265 **6**, 620–624 (2020).

266 20. U. Nagalakshmi, N. Meier, J.-Y. Liu, D. F. Voytas, S. P. Dinesh-Kumar, High-efficiency
267 multiplex biallelic heritable editing in Arabidopsis using an RNA virus. *Plant Physiol.* **189**,
268 1241–1245 (2022).

269 21. Y. Qi, Y. Zhang, F. Zhang, J. A. Baller, S. C. Cleland, Y. Ryu, C. G. Starker, D. F. Voytas,
270 Increasing frequencies of site-specific mutagenesis and gene targeting in Arabidopsis by
271 manipulating DNA repair pathways. *Genome Res.* **23**, 547–554 (2013).

272 22. I. W. Badon, Y. Oh, H.-J. Kim, S. H. Lee, Recent application of CRISPR-Cas12 and OMEGA
273 system for genome editing. *Mol. Ther.* **32**, 32–43 (2024).

274 23. S. A. Macfarlane, Tobraviruses--plant pathogens and tools for biotechnology. *Mol. Plant Pathol.*
275 **11**, 577–583 (2010).

276 24. C. Zhang, S. Liu, X. Li, R. Zhang, J. Li, Virus-Induced Gene Editing and Its Applications in
277 Plants. *Int. J. Mol. Sci.* **23** (2022).

278 25. C. LeBlanc, F. Zhang, J. Mendez, Y. Lozano, K. Chatpar, V. F. Irish, Y. Jacob, Increased
279 efficiency of targeted mutagenesis by CRISPR/Cas9 in plants using heat stress. *Plant J.* **93**, 377–
280 386 (2018).

281 26. Z. Li, Z. Zhong, Z. Wu, P. Pausch, B. Al-Shayeb, J. Amerasekera, J. A. Doudna, S. E. Jacobsen,
282 Genome editing in plants using the compact editor CasΦ. *Proc. Natl. Acad. Sci. U. S. A.* **120**,
283 e2216822120 (2023).
284

285 **Acknowledgments:**

286 **Funding:** This work was supported by an NSF Plant Genome Research Program grant to
287 SEJ, JAD and JFB. SEJ and JAD are Investigators of the Howard Hughes Medical Institute.
288 H.S. is an HHMI Fellow of The Jane Coffin Childs Fund for Medical Research. B.A.A. is
289 supported by m-CAFEs Microbial Community Analysis & Functional Evaluation in Soils, a
290 Science Focus Area led by Lawrence Berkeley National Laboratory based upon work
291 supported by the US Department of Energy, Office of Science, Office of Biological &
292 Environmental Research (DE-AC02-05CH11231). We thank Suhua Feng, Mahnaz Akhavan
293 and the Broad Stem Cell Research Center Biosequencing Core for sequencing support;
294 Colette Picard for assistance with analysis of amplicon sequencing data; Dinesh Kumar for
295 supplying the TRV2 plasmid pDK3888; Feng Zhang for providing the *ku70* (SALK123114)
296 mutant; and all members of the Jacobsen lab for their helpful insight and suggestions.
297

298 **Author contributions:**

299 TW, MK, HS, ZL, BAA, JB, JAD and SEJ designed the research
300 TW, HS, JAD, and SEJ interpreted the data
301 TW and SEJ wrote the manuscript

HS and KV performed bacterial interference assay
TW, MK, HS, KV, and ZL designed and built plasmids
TW, MK, ZL, JA, MS, GW, SC, CA, NS, and AS performed protoplast experiments
TW, MK, MS, GW, SC, CA, NS, AS, and DS performed transgenic *Arabidopsis* editing experiments
TW, MK, MS, GW, SC, CA, NS, AS, and DS performed TRV delivery experiments

Competing interests: T.W., M.K, J.A, Z.L, H.S, B.A.A., J.A.D. and S.E.J. have filed a patent covering aspects of this work.

Data and materials availability: All amp-seq data generated in this study are accessible at NCBI Sequence Read Archive under BioProject PRJNA1124592.

Supplementary Materials:
References only cited in the SM:

25. C. LeBlanc, F. Zhang, J. Mendez, Y. Lozano, K. Chatpar, V. F. Irish, Y. Jacob, Increased efficiency of targeted mutagenesis by CRISPR/Cas9 in plants using heat stress. *Plant J.* **93**, 377–386 (2018).

26. Z. Li, Z. Zhong, Z. Wu, P. Pausch, B. Al-Shayeb, J. Amerasekera, J. A. Doudna, S. E. Jacobsen, Genome editing in plants using the compact editor CasΦ. *Proc. Natl. Acad. Sci. U. S. A.* **120**, e2216822120 (2023).

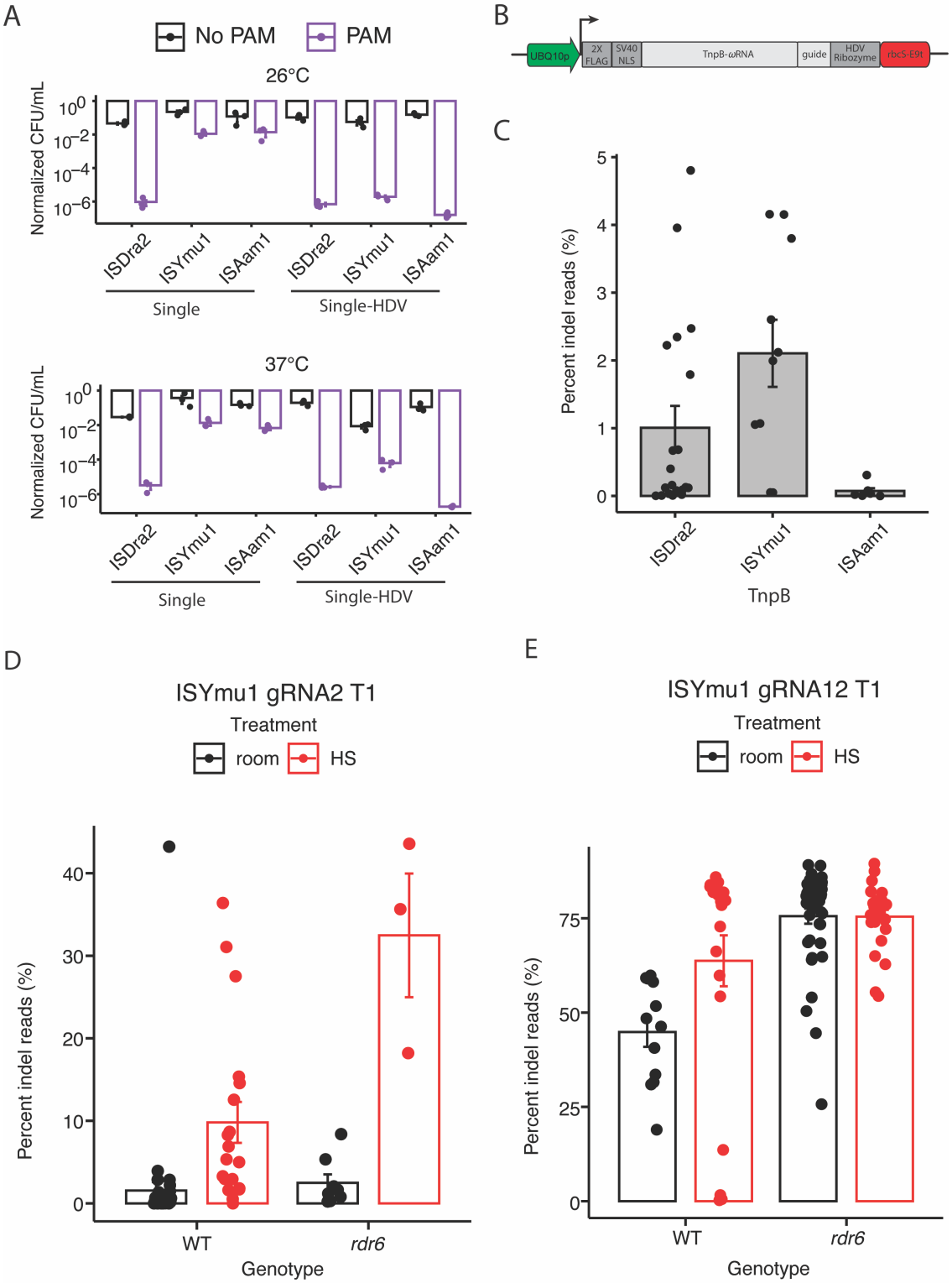

Fig. 1. Expression of TnpB and guide RNA in a single transcript for plant genome editing. (A) Barplots displaying interference assay testing the single transcript expression TnpB vectors for cleavage in E. coli. The barplot on the top displays data from experiments performed at 26°C and the barplot below depicts data from experiments performed at 37°C. Black bars indicate absence of a PAM on the target plasmid and purple bars indicate the presence of a PAM on the target plasmid. The Y-axis is a log10 scale of the normalized colony forming units

330 (CFU)/milliliter (mL). The X-axis displays the three TnpBs tested using the single expression
331 transcript design without an HDV ribozyme or the single expression design with an HDV
332 ribozyme. The standard error of the mean (SEM) was calculated for each experiment. **(B)**
333 Schematic of the single expression transcript plasmid design used for plant genome editing. The
334 green arrow symbolizes the At*UBQ10* promoter; dark gray boxes indicate the 2X-FLAG, SV40
335 NLS and HDV ribozyme sequences; light gray boxes indicate the TnpB-ωRNA and guide
336 sequences; red box symbolizes the rbcS-E9 terminator; and the black arrow indicate the
337 orientation of the TnpB-ωRNA expression cassette. **(C)** Barplot displaying the average editing
338 frequency for protoplast experiments using ISDra2, ISYmu1 and ISAam1. Each dot represents
339 the average editing efficiency of a gRNA from Fig. S3A. The Y-axis indicates the editing
340 efficiencies (percent indel reads (%)). The X-axis displays the ISDra2, ISYmu1 and ISAam1
341 TnpBs tested. The standard error of the mean (SEM) was calculated for each experiment. **(D-E)**
342 ISYmu1 somatic editing in T1 transgenic plants. Panels D and E display a barplot for ISYmu1
343 gRNA2 and ISYmu1 gRNA12, respectively. Each dot indicates a single T1 transgenic plant. The
344 room and HS treatments stand for room temperature and heat shock plant growth conditions,
345 respectively. The genotypes are plotted along the X-axis and the editing efficiencies (percent
346 indel reads (%)) are plotted on the Y-axis. The standard error of the mean (SEM) was calculated
347 for each experiment. WT is an abbreviation for wild type, and *rdr6* is an abbreviation for a
348 mutation in the *RNA-DEPENDENT RNA POLYMERASE 6* gene.
349

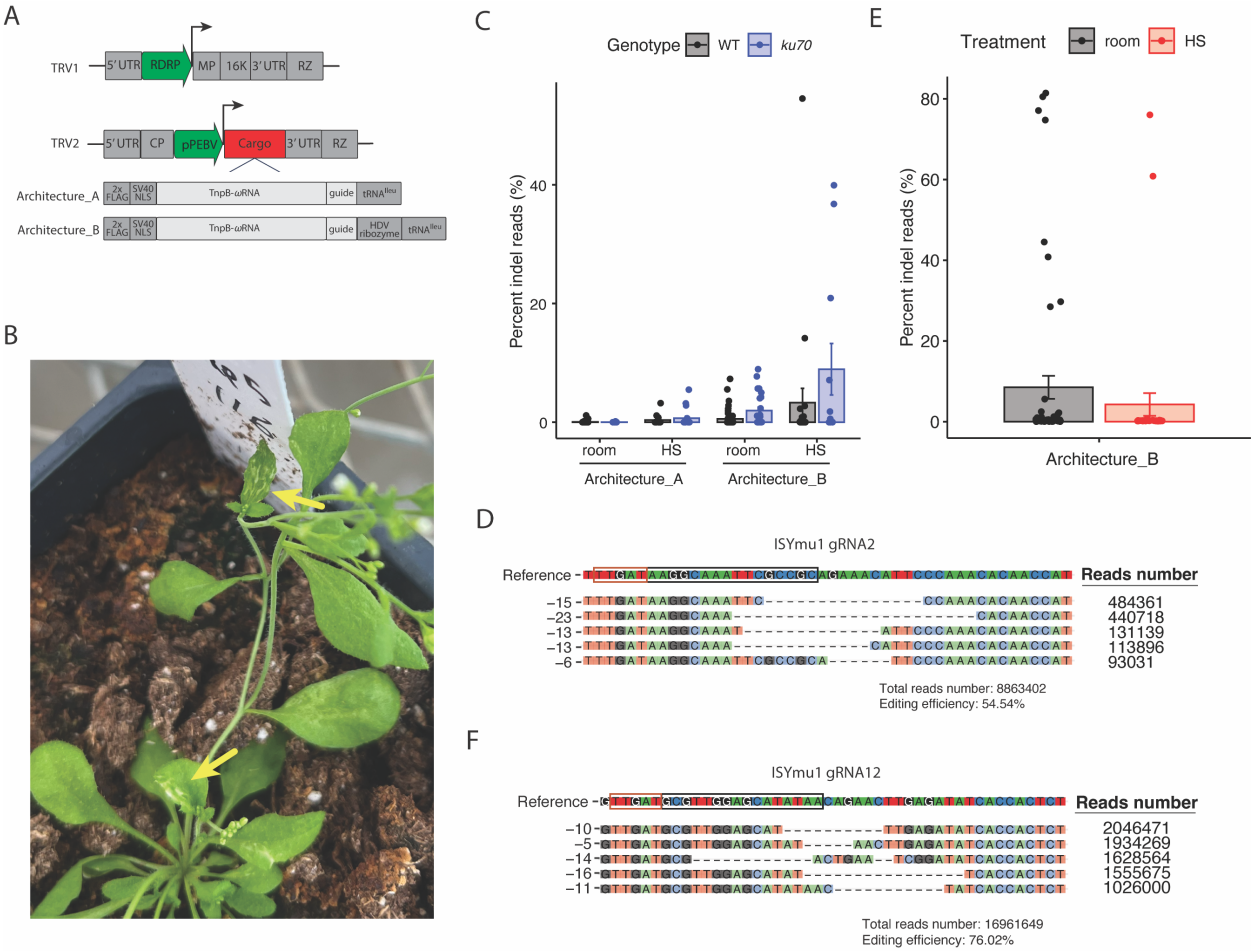

Fig. 2. Somatic editing of *Arabidopsis* using TRV to deliver ISYmu1 TnpB and guide RNA. **(A)** Schematic of the TRV1 and TRV2 plasmids. Green arrows indicate the RNA dependent RNA polymerase (RDRP) and pea early browning virus (pPEBV) promoters for TRV1 and TRV2, respectively; gray boxes in TRV1 and TRV2 indicate the native TRV components; the red Cargo box in TRV2 indicates the location of either Architecture_A or Architecture_B; below TRV2 are schematics of Architecture_A and Architecture_B **(B)** Representative picture of a plant displaying white sectors three weeks after TRV delivery. Yellow arrows indicate leaves containing white sectors. **(C)** Barplot displaying the somatic editing for ISYmu1 gRNA2 in wild type (WT) and *ku70* genetic backgrounds. WT samples are black and *ku70* samples are blue. The TRV2 Cargo Architectures are plotted along the X-axis with either room temperature (room) or heat shock (HS) growth conditions. The Y-axis indicates the editing efficiencies (percent indel reads (%)). Each dot represents an individual plant that underwent agroflood TRV delivery. The standard error of the mean (SEM) was calculated for each experiment. **(D)** DNA insertion or deletion (indel) repair profile for an individual WT plant that underwent delivery of TRV Cargo Architecture_B with ISYmu1 gRNA2 under the heat shock treatment. The top five most common indel types are listed on the left. The read counts for each indel are listed on the right. The PAM is identified by the red box, and the target site is outlined by the black box, in the Reference sequence. The total read number and editing efficiency are listed below the indel profile. **(E)** Barplot displaying the somatic editing for ISYmu1gRNA12 in wild type (WT). Room temperature treatment (room) samples are black and heat shock (HS) samples are red. The TRV2 Cargo Architecture_B is plotted along the X-axis. The Y-axis indicates the editing efficiencies (percent indel reads (%)). Each dot represents an individual plant that underwent

373 agroflood TRV delivery. The standard error of the mean (SEM) was calculated for each
374 experiment. **(F)** DNA indel repair profile for an individual WT plant that underwent delivery of
375 TRV Cargo Architecture_B with ISYmu1 gRNA12 under the heat shock treatment. The top five
376 most common indel types are listed on the left. The read counts for each indel are listed on the
377 right. The PAM is identified by the red box, and the target site is outlined by the black box, in
378 the Reference sequence. The total read number and editing efficiency are listed below the indel
379 profile.
380

A

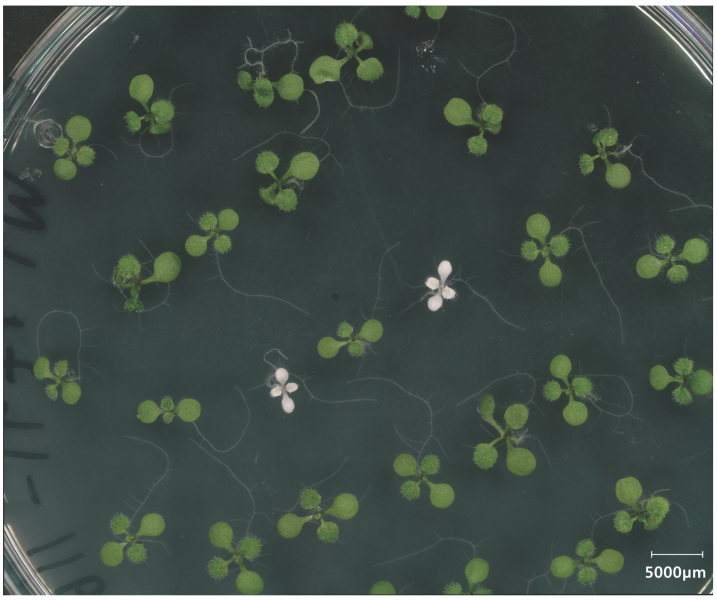

B

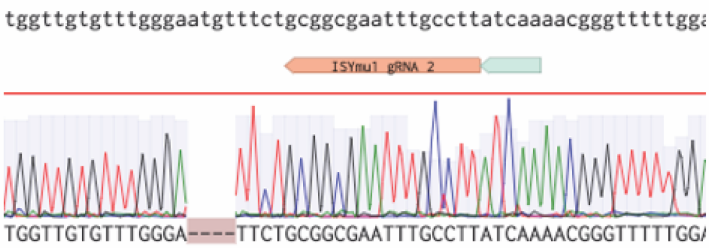

Fig. 3. Inheritance of edited alleles from a TRV-infected plant. (A) Representative image of albino and green progeny seedlings from a WT plant showing 54.54% somatic editing using the TRV2 Architecture_B design with gRNA2 that underwent heat shock treatment. **(B)** Sanger sequencing trace file screenshot from one of the albino plants in Fig. 3A. The sequence at the top is the wild type reverse complement; below that are the ISYmu1 gRNA2 target and PAM (gray box) identifiers; the .ab1 trace file displays a homozygous 4bp deletion.

Supplementary Materials for

Title: Viral delivery of an RNA-guided genome editor for transgene-free plant germline editing

Authors: Trevor Weiss[1], Maris Kamalu[1], Honglue Shi[2,6], Zheng Li[1], Jasmine Amerasekera[1], Benjamin A. Adler[2,3], Michelle Song[1], Kamakshi Vohra[2,11], Gabriel Wirnowski[1], Sidharth Chitkara[1], Charlie Ambrose[1], Noah Steinmetz[1], Ananya Sridharan[1], Diego Sahagun[1], Jillian F. Banfield[2,8,9,10], Jennifer A. Doudna[2,4,6,11,12,13,14], Steven. E. Jacobsen[1,7,15*]

*Corresponding author. Email: jacobsen@ucla.edu

The PDF file includes:

Materials and Methods
Figs. S1 to S4
Tables S1 to S7

Materials and Methods:

Plasmids used in this study

Plasmids used for bacterial assay were generated as follows. The single expression cassette containing TnpB and ωRNA DNA sequences were synthesized as geneblocks from IDT (Integrated DNA Technologies), and golden-gate cloned using BsmbI restriction enzyme (cat E1602S) into a vector (chloramphenicol (Cam) resistance) under a single tetracycline-inducible promoter (TetR/pTet) to make the TnpB-ωRNA plasmid. Target sites with various PAM sequences and target sites were golden-gate cloned with BbsI restriction enzyme (cat R3539S) into a vector (ampicillin (Amp) /carbenicillin (Carb) resistance).

Plasmids were generated for protoplast and floral dip experiments using a two-step cloning strategy. In step one, the ISDra2, ISYmu1, and ISAam1 protein coding and ωRNA DNA sequences were synthesized as geneblocks by IDT (Integrated DNA Technologies). Then, starting with the pC1300_pUB10_pcoCASphi_E9t_MCS_version2 vector (*26*), we used PCR and NEBuilder HiFi DNA Assembly (cat E2621) to assemble the TnpB-ωRNA geneblocks into plant expression vectors with a toxic *ccdB* insert flanked by PaqCI sites immediately downstream of the ωRNA scaffold and preceding an HDV ribozyme sequence. The HiFi reactions were then transformed into One Shot *ccdB* Survival 2 T1R Competent Cells (cat A10460) to obtain the pMK003 (ISDra2), pMK025 (ISYmu1), and pMK024 (ISAam1) intermediate vectors for facile guide sequence cloning (table S3). In step two, guide sequences were synthesized as individual top and bottom strands with 4 base pair (bp) overhangs from IDT, phosphorylated and annealed, and then used for golden-gate assembly using the NEB PaqCI enzyme (cat R0745) (table S4). When transformed into NEB 10-beta Competent E. coli (cat C3019), vectors that still contained the *ccdB* gene would kill the cells, leaving behind only the transformants possessing successfully assembled TnpB plant expression vectors harboring a guide RNA (gRNA) sequence.

TRV2 vectors were created with the pDK3888 plasmid as a base vector (*20*). NEBuilder HiFi DNA Assembly (cat E2621) was used to clone the ISYmu1 gRNA2 Architecture_A, ISYmu1 gRNA2 Architecture_B, and ISYmu1 gRNA12 Architecture_B into the TRV2 cargo slot. First, pDK3888 was digested using NEB ZraI (cat R0659), NEB PmlI (cat R0532), and NEB Quick CIP (cat M0525) overnight, and purified using Qiagen QiaQuick purification column (cat 28104). Next, three PCR reactions were performed to amplify the fragments needed for NEBuilder HiFi DNA Assembly, followed by purification using Qiagen QiaQuick purification column (cat 28104) (table S5). The digested and purified pDK3888 plasmid and purified PCR fragments were used to assemble the final TRV2 plasmid using NEBuilder HiFi DNA Assembly according to the manufacturer's instructions. Finally, the NEBuilder HiFi DNA Assembly reaction was transformed into NEB 10-beta Competent E.coli (cat C3019). Correct plasmids were confirmed using Primordium whole plasmid sequencing. A list of all plasmids used in this research can be found in table S3.

Bacterial interference assay

For the bacterial interference assay, we co-transfected 100 ng of the TnpB-ωRNA plasmid and 100 ng of the target plasmid to 33 µl of NEB 10-beta electrocompetent E. coli cells (catC3020K). Specifically, the target plasmid contains a target site either flanking the canonical PAM (TTGAT for ISYmu1 and ISDra2 and TTTAA for ISAam1) or flanking a non-canonical PAM (GGGGG). The cells were recovered in 1 mL of NEB 10-Beta Stable/Outgrowth media (cat B9035S) for 1 hour. Following recovery, a series of 5-fold dilutions of the recovery culture

were prepared. Each dilution (5 µL) was spot-plated onto LB-Agar plates containing double antibiotics (34 µg/mL chloramphenicol, 100 µg/mL carbenicillin, and 2 nM anhydrotetracycline) and onto control plates with a single antibiotic (34 µg/mL chloramphenicol and 2 nM anhydrotetracycline). If no colonies were visible on the serial dilution plates, 400 µL of the 1 mL recovery culture was plated entirely on the double antibiotic plate to enhance detection sensitivity. Plates were left overnight at either 26°C or 37°C, and colony-forming units (CFU) were counted on all plates the next morning. The normalized CFU were calculated by taking the ratio of CFU on the double antibiotic plates to the CFU on the single antibiotic plates. The normalized CFU in the canonical PAM conditions were compared to the one in the non-canonical PAM conditions. Experiments were performed in triplicate.

Plant materials and growth conditions

For protoplast preparation, *Arabidopsis* Columbia ecotype (Col-0) seeds were suspended in a 0.1% agar solution and kept at 4°C in the dark for three days to stratify. Following stratification, seeds were planted on Jiffy pucks and grown under a 12-h light/12-h dark photoperiod, with low light condition for 3 to 4 weeks (*16*).

The *Arabidopsis* Col-0 ecotype was used in these experiments. The *rdr6* genotype was created in the Steve Jacobsen Lab using CRISPR-Cas9, resulting in a 616 bp deletion in the gene body of *rdr6*. The *ku70* (SALK_123114) genotype was provided from Feng Zhang at the University of Minnesota. Floral dip transformation was performed according to the protocol as previously outlined using the Agl0 agrobacterium strain (*17*). Transgenic T1 plants were screened using ½ MS plates with 40 µg/mL hygromycin B under a 16-/8-h light/dark cycle at 23°C. After one week, transgenic seedlings that passed selection were transferred to soil and moved to a greenhouse (23°C).

For agroflood experiments, sterilized seeds were sown on ½ MS agar plates and stratified for five days. After five days, the seeds were moved to a growth room and grown under a 16-/8-h light/dark cycle at 23°C for 8-10 days. The seedlings were then used for TRV delivery using agroflood (*20*).

A subset of transgenic T1 plants, and plants that underwent agroflood, were subjected to a heat shock treatment modified from LeBlanc et al. (*25*). Seedlings that passed hygromycin selection, or underwent agroflood, were transplanted to soil and grown in a greenhouse (23°C) for one week. After one week, plants that did not receive a heat shock treatment continued to grow in the greenhouse (23°C); however, plants that underwent heat shock treatment were exposed to eight hours (9am - 5pm) of heat exposure at 37°C every day for 5 days, followed by 2 days of recovery in a greenhouse (23°C). This heat shock regime lasted for two weeks.

Protoplast isolation and transfection

Arabidopsis mesophyll protoplast isolation was performed as previously described (*16*). Plasmid transfections into *Arabidopsis* protoplasts were performed using 20 µg of plasmid, similarly as Li et al. (*26*). The concentrations of plasmids were determined by nanodrop. Plasmids were added to the bottom of each transfection tube, and the volume of the plasmid was supplemented with water to reach 20 µl. 200 µl of protoplasts were added followed by 220 µl of fresh and sterile polyethylene glycol (PEG)-CaCl2 solution. The samples were mixed by gently tapping the tubes, and incubated at room temperature for ten minutes. After ten minutes, 880 µl of W5 solution was added and mixed with the protoplasts by inverting the tube two to three times to stop the transfection. Next, protoplasts were harvested by centrifuging the tubes at 100

139 relative centrifugal force (RCF) for 2 min and resuspended in 1 mL of WI solution. The
140 protoplast cells were then plated in 6-well plates pre-coated with 5% calf serum. Protoplast cells
141 in the 6-well plates were incubated at 26°C for 48 hours. During the 48 hour incubation, the
142 protoplast cells were subjected to a 37°C heat shock treatment for 2 hours at 16 hours post
143 transfection. At 48 hours post transfection, protoplasts were harvested for genomic DNA
144 extraction.
145
146 TRV delivery to *Arabidopsis* seedlings
147 TRV delivery was performed as previously described in Nagalakshmi et al (*20*). TRV1
148 and TRV2 vectors were first introduced into the GV3101 agrobacterium strain. The
149 agrobacterium harboring TRV vectors were grown in 200 mL of lysogeny broth (LB) with
150 antibiotics for 18 hours at 28°C. Agrobacterium cultures were centrifuged for twenty minutes at
151 3500 RCF. The LB was discarded and the agrobacterium cells were resuspended in 150 mL of
152 sterile water. The resuspended agrobacterium was centrifuged for ten minutes at 3500
153 revolutions per minute (RPM). The supernatant was discarded and the pellet was resuspended in
154 sterile agro-infiltration buffer containing 10 mM MgCl2, 10 mM 2-(N-morpholino)
155 ethanesulfonic acid, and 250 µM acetosyringone to OD_{600} = 1.5. The agrobacterium cells were
156 then incubated at 23°C for three hours with slow shaking. After three hours, the agrobacterium
157 harboring TRV1 and TRV2 were mixed in a 1:1 ratio. 15 mL of the 1:1 ratio of TRV was
158 delivered to 8-10 day old seedlings. After four days of agroflood co-culture, seedlings were
159 transplanted to soil.
160
161 Screening progeny from an agroflooded plant
162 Seeds were harvested from the TRV-infected plant that displayed 54.54% somatic editing
163 about 12 weeks after TRV delivery. The seeds sown on ½ MS plates supplemented with 3%
164 sucrose and stored at 4°C in the dark for five days to stratify. After five days, the seeds were
165 moved to a growth room and grown under a 16-/8-h light/dark cycle at 23°C for 10-12 days.
166 Next Generation amplicon sequencing, Sanger sequencing, or RT-Polymerase Chain Reaction
167 (PCR) was then performed on a subset of the progeny plants.
168
169 Amplicon sequencing
170 DNA was extracted from protoplast samples using Qiagen DNeasy plant mini kit (Qiagen
171 69106). Tissue was collected from transgenic T1 plants by sampling and pooling leaf tissue from
172 three random leaves on a single plant three weeks after being transplanted to soil. For the plants
173 that underwent agroflood, leaf tissue was sampled by collecting and pooling tissue from three
174 random (however, if white sectors were visible that leaf was sampled) leaves on a single plant
175 distal to the TRV delivery site three weeks after being transplanted to soil. Once tissue samples
176 were collected, they were frozen at -80°C overnight. The samples were then ground and DNA
177 was extracted using invitrogen Platinum Direct PCR Universal Master Mix (refA44647500)
178 according to the manufacturer's instructions. For the progenies of the plant that underwent
179 agroflood, a single leaf tissue was sampled and DNA was extracted using invitrogen Platinum
180 Direct PCR Universal Master Mix (REF A44647500) according to the manufacturer's
181 instructions. The DNA was then used for Next Generation amplicon sequencing.
182 As similarly performed in Li et al. (*26*), editing efficiency was characterized using single-
183 end Next Generation Sequencing on the Illumina NovaSeqX platform. Libraries were prepared
184 via a 2-step PCR amplification method. In the first round of amplification, each target site was

185 amplified using primers flanking the target site (table S6). After 25 cycles of amplification, the
186 reactions were cleaned using a 1.0X Ampure XP bead purification (Beckman Coulter A63881).
187 Next, each sample went through 12 additional cycles of amplification using Illumina indexing
188 primers. The samples were cleaned using 0.7X Ampure XP bead purification (Beckman Coulter
189 A63881). Samples were checked for purity on a 2% agarose gel, quantified using Nanodrop,
190 normalized, and pooled.
191
192 Amplicon sequencing analysis
193 Amplicon sequencing analysis was performed similarly as Li et al (*26*). Reads were
194 adapter trimmed using Trim Galore default settings. Reads were mapped to the target genome
195 region using the BWA aligner (v0.7.17, BWA-MEM algorithm). Sorted and indexed bam files
196 were used as input for further analysis by the CrispRvariants R package (v1.14.0). Each mutation
197 pattern with corresponding read counts was exported by the CrispRvariants R package. Only
198 reads with a >= 3 bp deletion or insertion (indel) of the same type with >=10 read counts from a
199 sample were counted as edited reads. SNVs were also filtered out.
200
201 RT-PCR
202 Total RNA from TRV-infected progeny plants was extracted using Zymo Research
203 Direct-zol RNA MiniPrep kit (cat R2052). Total RNA was converted to cDNA using the
204 invitrogen SuperScript IV VILO Master Mix (cat 11766050). RT-PCR control was performed
205 using primers targeting the *AtIPP2* gene (table S7). PCR was performed to check for the
206 presence/absence of the TRV vector using SP9238 and SP9239 as previously described in
207 Nagalakshmi et al (table S7) (*20*). PCR was performed using New England Biolabs Q5 High-
208 Fidelity 2X Master Mix (cat M0492L) according to the manufacturer's instructions, using 2 µl of
209 cDNA in a 25 µl reaction. PCR conditions included a 98°C initial denaturation step for 30
210 seconds, 35x(98°C, 10 sec; 55°C, 20 sec; 72°C, 10 sec), 72°C for 2 min. 10 µl of the PCR
211 reactions were analyzed by 2% agarose gel electrophoresis.
212
213
214
215
216
217

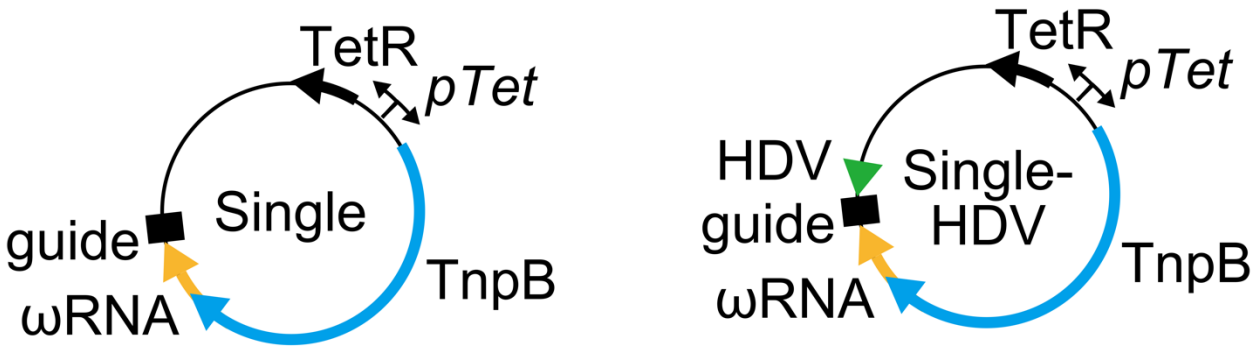

Fig. S1. Schematic of interference assay plasmids containing either the TnpB-ωRNA Single or TnpB-ωRNA Single-HDV design. The blue arrow indicates the TnpB sequence; the yellow arrow indicates the ωRNA sequence; the black rectangle indicates the guide sequence; the green arrow indicates the HDV ribozyme sequence. The plasmids contain the tetracycline resistance gene (TetR). A tetracycline promoter (pTet) was used to drive expression of the TnpB-ωRNA single or Single-HDV sequences, and the tetracycline resistance gene.

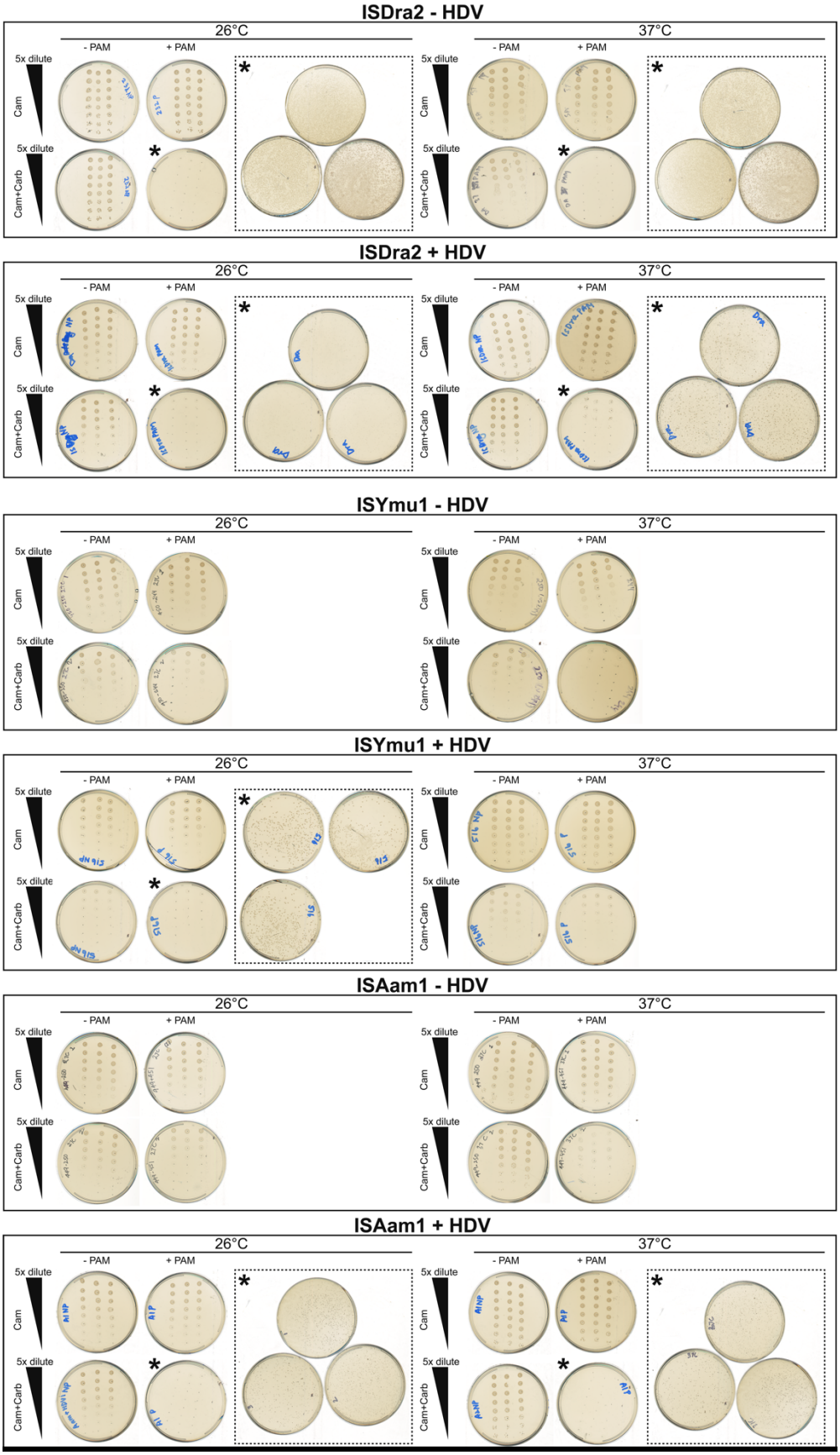
ISDra2 - HDV
26°C
37°C
- PAM
+ PAM
5x dilute
Cam
Cam+Carb
ISDra2 + HDV
ISYmu1 - HDV
ISYmu1 + HDV
ISAam1 - HDV
ISAam1 + HDV

226

227 **Figure S2: The plate images of bacterial plasmid interference assay.** Five-fold serial
228 dilutions (5 μL) from the 1 mL recovery culture post transformation were plated on both single
229 antibiotic LB-Agar plates (Cam, upper row) and double antibiotic LB-Agar plates (Cam+Carb,
230 lower row). Plates without visible colonies (indicated by an asterisk) had 400 μL of the original 1
231 mL recovery culture plated on the double antibiotic plates (dash insets). Experiments were
232 performed in triplicates.

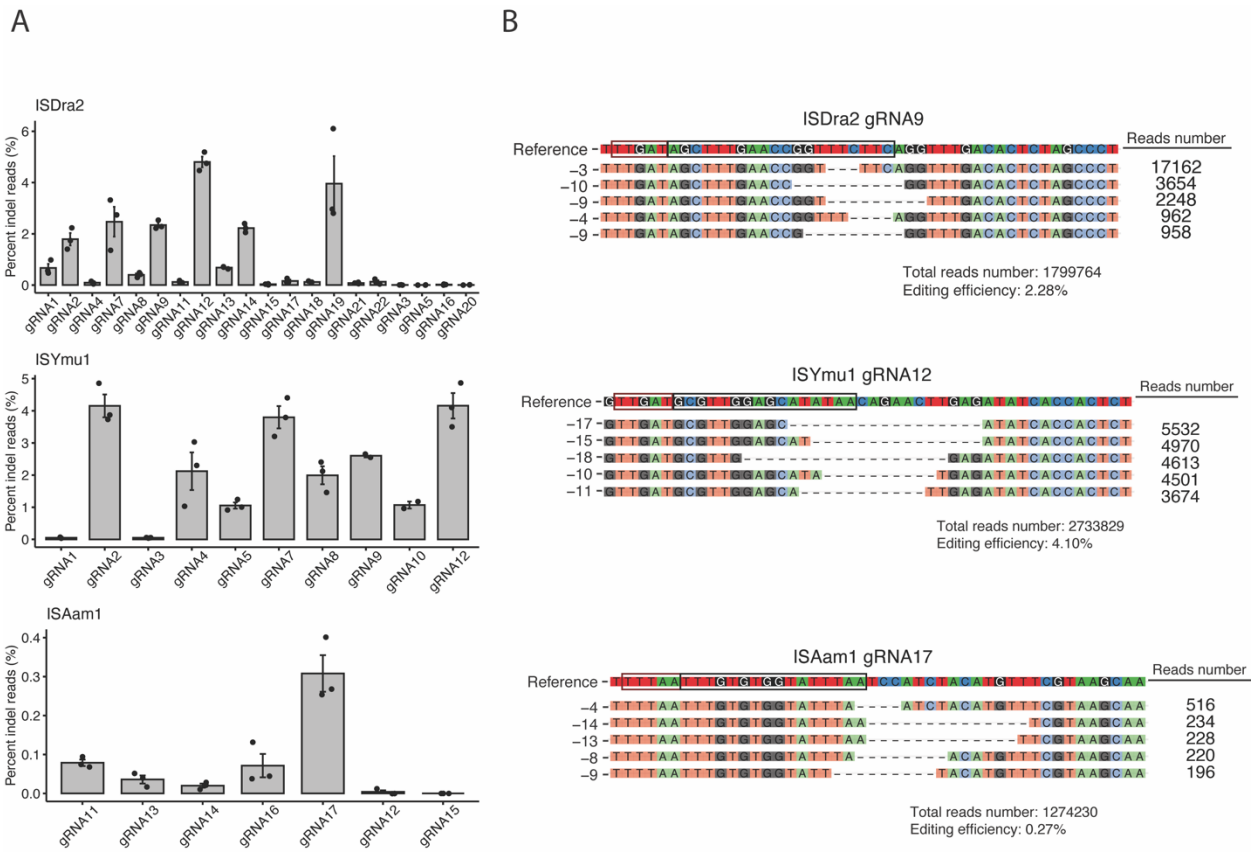

Fig. S3. Editing efficiency and repair profiles for ISDra2, ISYmu1 and ISAam1 in *Arabidopsis* protoplast experiment. (A) Barplots displaying the editing efficiency of individual gRNAs for each TnpB tested. The name of the TnpB is at the upper left of each barplot. The gRNAs are plotted along the X-axis and the editing efficiency (percent indel reads (%)) is plotted on the Y-axis. Each dot indicates a single transfection. The standard error of the mean (SEM) was calculated for each target site. **(B)** DNA repair indel profiles for individual transfection samples. The top five most common indel types are listed on the left. The read counts for each indel are listed on the right. The PAM is identified by the red box, and the target site is outlined by the black box, in the Reference sequence. The total read number and editing efficiency are listed below each indel profile. The name of each TnpB and gRNA is displayed above the reference sequence of each indel repair profile.

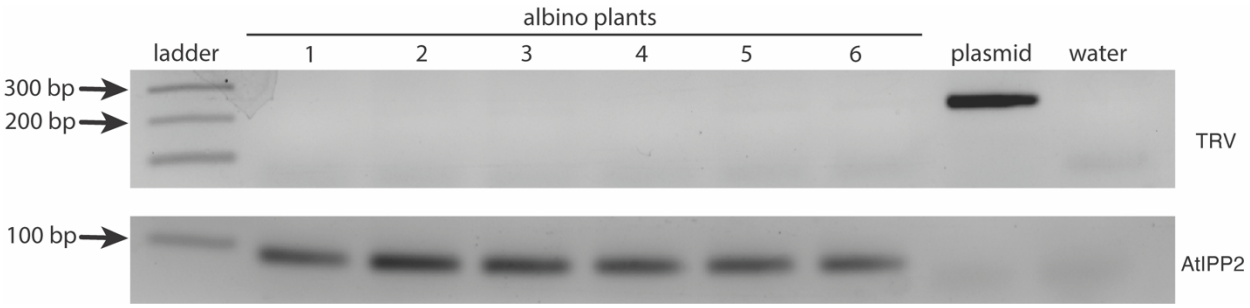

Fig. S4. RT-PCR gel showing absence of the TRV in the progeny of a TRV-infected plant. RT-PCR was performed using total RNA extracted from albino plants homozygous for a 4 bp deletion at the *AtPDS3* gene. Gel electrophoresis image for RT-PCR using primers targeting TRV (upper panel) and *AtIPP2* gene (bottom panel). The lanes are indicated (from left to right) as ladder, six individual albino plants, plasmid control, and a water control. Black arrows indicate the amplicon size.

254 **Table S1. ISDra2, ISYmu1 and ISAam1 target sites.** The table consists of four columns. The
255 TnpB and Guide columns indicate the TnpB and gRNA used. The gRNA sequence column lists
256 the gRNA sequence used for targeted genome editing. The Genomic location column provides
257 the location of each gRNA target site in the *Arabidopsis* genome.
258

TnpB	Guide	gRNA sequence	Genomic location
ISDra2	gRNA1	ttacgaattgatgaccatat	4:8195186-8195206
ISDra2	gRNA2	aaggcaaattcgccgcagaa	4:8194730-8194749
ISDra2	gRNA3	tcacattaagcctagaaact	4:8193921-8193940
ISDra2	gRNA4	cccaagttctccaaataaat	4:8193476-8193495
ISDra2	gRNA5	tacccatcctaaagtatggg	4:8192944-8192963
ISDra2	gRNA7	aaattcaacatctttctcta	4:8190835-8190854
ISDra2	gRNA8	tggtctcactttccgaatta	4:8194167-8194186
ISDra2	gRNA9	agctttgaaccggtttcttc	4:8192305-8192324
ISDra2	gRNA11	cgaaaactgaagaacacata	4:8191494-8191513
ISDra2	gRNA12	gcgttggagcatataacaga	4:8195556-8195575
ISDra2	gRNA13	taaagagaggaaattgcagg	4:8194513-8194532
ISDra2	gRNA14	ggtagagctgataagatata	4:8193625-8193644
ISDra2	gRNA15	aaaattggattaatgtgcac	4:8193203-8193222
ISDra2	gRNA16	tactattaaatgtcaaaatc	4:8193077-8193096
ISDra2	gRNA17	caatacaaataaatacatgc	4:8193117-8193136
ISDra2	gRNA18	caattcaagctaattataga	4:8193095-8193114
ISDra2	gRNA19	gagcttaacttggtagagta	4:8192577-8192596
ISDra2	gRNA20	ttgtcagctttcttatggat	4:8192528-8192547
ISDra2	gRNA21	gttgattaacttgtactacc	4:8192131-8192150
ISDra2	gRNA22	taacttgtactacctcatcc	4:8192125-8192144
ISYmu1	gRNA1	ttacgaattgatgacc	4:8195187-8195202
ISYmu1	gRNA2	aaggcaaattcgccgc	4:8194730-8194745
ISYmu1	gRNA3	tcacattaagcctaga	4:8193921-8193936
ISYmu1	gRNA4	cccaagttctccaaat	4:8193476-8193491
ISYmu1	gRNA5	tacccatcctaaagta	4:8192944-8192959
ISYmu1	gRNA7	aaattcaacatctttc	4:8190839-8190854
ISYmu1	gRNA8	tggtctcactttccga	4:8194171-8194186
ISYmu1	gRNA9	agctttgaaccggttt	4:8192309-8192324
ISYmu1	gRNA10	taacttgtactacctc	4:8192129-8192144
ISYmu1	gRNA12	gcgttggagcatataa	4:8195560-8195575
ISAam1	gRNA11	caattcatctggtatc	4:8191755-8191770
ISAam1	gRNA12	ccaagaacaagcctta	4:8191347-8191362
ISAam1	gRNA13	gttttgtcctcttctc	4:8190412-8190427
ISAam1	gRNA14	caatttacctatctta	4:8193797-8193812

ISAam1	gRNA15	cacataattgaaaaga	4:8194919-8194934
ISAam1	gRNA16	aatttgttacacaact	4:8195755-8195770
ISAam1	gRNA17	tttgtgtggtatttaa	4:8195158-8195173

259

260 **Table S2. Phenotype and genotype of the progenies from a TRV-infected plant.** The Sample
261 column indicates an internal identifier for each plant sampled. The Phenotype column indicates
262 whether the plant was green (WT) or albino. The Genotype (allele1 / allele2) column lists the
263 alleles of the *AtPDS3* gene determined by amp-seq. WT is an abbreviation for wild type, bp is an
264 abbreviation for base pair, and del is an abbreviation for deletion.

Sample	Phenotype	Genotype (allele1 / allele2)
1	Albino	4bp del / 4bp del
2	Albino	4bp del / 4bp del
3	WT	WT / WT
4	WT	WT / WT
5	WT	4bp del / WT
6	WT	WT / WT
9	WT	WT / WT
10	WT	WT / WT
12	WT	WT / WT
13	WT	WT / WT
14	WT	WT / WT
15	WT	WT / WT
16	WT	WT / WT
17	WT	WT / WT
18	WT	WT / WT
19	WT	WT / WT
20	WT	WT / WT
21	WT	WT / WT
22	WT	WT / WT
23	WT	WT / WT
24	WT	WT / WT
25	WT	WT / WT
26	WT	WT / WT
27	WT	WT / WT
28	WT	4bp del / WT
29	WT	WT / WT
30	Albino	4bp del / 4bp del
31	Albino	4bp del / 4bp del
32	Albino	4bp del / 4bp del
33	Albino	4bp del / 4bp del
34	Albino	4bp del / 4bp del
35	Albino	4bp del / 4bp del
36	Albino	4bp del / 4bp del

38	Albino	4bp del / 4bp del
39	Albino	4bp del / 4bp del
40	Albino	4bp del / 4bp del
41	Albino	4bp del / 4bp del
42	Albino	4bp del / 4bp del
43	Albino	11 bp del / 17bp del
45	Albino	4bp del / 4bp del
46	Albino	4bp del / 4bp del
47	Albino	4bp del / 4bp del
48	Albino	4bp del / 4bp del
49	Albino	10bp del / 12 bp del
50	Albino	4bp del / 4bp del
51	Albino	4bp del / 4bp del
52	Albino	4bp del / 4bp del
53	Albino	4bp del / 4bp del
54	Albino	4bp del / 4bp del
56	Albino	4bp del / 4bp del
57	Albino	4bp del / 4bp del
58	Albino	4bp del / 4bp del
59	Albino	4bp del / 4bp del
60	Albino	4bp del / 4bp del
61	Albino	4bp del / 4bp del
65	Albino	4bp del / 4bp del
72	Albino	4bp del / 4bp del
79	Albino	4bp del / 4bp del
80	Albino	4bp del / 4bp del
84	Albino	4bp del / 4bp del
85	Albino	4bp del / 4bp del
86	Albino	4bp del / 4bp del
90	Albino	17bp del / 11bp del
91	Albino	4bp del / 4bp del
92	Albino	4bp del / 4bp del
94	WT	WT / WT
95	WT	WT / WT

96	WT	WT / WT
97	WT	WT / WT
98	WT	WT / WT
99	WT	WT / WT
100	WT	4bp del / WT
101	WT	WT / WT
102	WT	WT / WT
103	WT	WT / WT
104	WT	WT / WT
105	WT	WT / WT
106	WT	WT / WT
107	WT	WT / WT
108	WT	4bp del / WT
109	WT	WT / WT
110	WT	WT / WT
111	WT	WT / WT
112	WT	WT / WT
113	WT	WT / WT
114	WT	WT / WT
115	WT	WT / WT
116	WT	WT / WT
117	WT	WT / WT
118	WT	WT / WT
119	WT	WT / WT
120	WT	WT / WT
122	WT	WT / WT
123	WT	WT / WT
124	WT	WT / WT
125	WT	WT / WT
126	WT	WT / WT
127	WT	WT / WT
129	WT	WT / WT
132	WT	WT / WT
133	WT	WT / WT

134	WT	WT / WT
135	WT	WT / WT
137	WT	WT / WT
138	WT	WT / WT
140	WT	WT / WT
141	WT	WT / WT
142	WT	WT / WT
143	WT	WT / WT
145	WT	WT / WT
147	WT	WT / WT
148	WT	WT / WT
149	WT	WT / WT
150	WT	WT / WT
151	WT	WT / WT
152	WT	WT / WT
153	WT	WT / WT
154	WT	WT / WT
156	WT	WT / WT
157	WT	WT / WT
158	WT	WT / WT
160	WT	WT / WT
161	WT	WT / WT
162	WT	WT / WT
163	WT	WT / WT
164	WT	WT / WT
165	WT	WT / WT
166	WT	WT / WT
167	WT	WT / WT
168	WT	WT / WT
169	WT	WT / WT
170	WT	WT / WT
171	WT	WT / WT
172	WT	WT / WT
173	WT	WT / WT

174	WT	WT / WT
175	WT	WT / WT
176	WT	WT / WT
177	WT	WT / WT
178	WT	WT / WT
179	WT	WT / WT
180	WT	4bp del / WT
181	WT	WT / WT
182	WT	WT / WT
183	WT	WT / WT
184	WT	WT / WT
185	WT	WT / WT
186	WT	WT / WT
187	WT	WT / WT
188	WT	WT / WT
189	WT	WT / WT
190	WT	WT / WT
191	WT	WT / WT
192	WT	WT / WT
193	WT	WT / WT
194	WT	WT / WT
195	WT	WT / WT
196	WT	WT / WT
198	WT	WT / WT
199	WT	WT / WT
200	WT	WT / WT
201	WT	WT / WT
202	WT	WT / WT
203	WT	WT / WT
204	WT	WT / WT
205	WT	WT / WT
206	WT	WT / WT
207	WT	WT / WT
208	WT	WT / WT

209	WT	WT / WT
210	WT	WT / WT
211	WT	WT / WT
212	WT	WT / WT
213	WT	WT / WT
214	WT	WT / WT
215	WT	4bp del / WT
216	WT	WT / WT
217	WT	4bp del / WT
218	WT	WT / WT
219	WT	WT / WT
220	WT	WT / WT
221	WT	WT / WT
222	WT	WT / WT
223	WT	WT / WT
224	WT	WT / WT
225	WT	WT / WT
226	WT	WT / WT
227	WT	WT / WT
228	WT	WT / WT
229	WT	WT / WT
230	WT	WT / WT
231	WT	WT / WT
232	WT	WT / WT
233	WT	WT / WT
234	WT	WT / WT
235	WT	WT / WT
236	WT	WT / WT
237	WT	WT / WT
238	WT	WT / WT
239	WT	WT / WT
240	WT	WT / WT
241	WT	WT / WT
242	WT	WT / WT

243	WT	WT / WT
244	WT	4bp del / WT
245	WT	WT / WT
246	WT	WT / WT
247	WT	WT / WT
248	WT	WT / WT

265

266 **Table S3. Plasmids used in this study.** The Plasmid column lists the name of each plasmid
267 used. The Description column provides a TnpB and gRNA description for each plasmid, along
268 with the intermediate plant expression vector that was used to create it.

Plasmid	Description
pMK003	Cloning vector for PaqCI Golden Gate assembly of ISDra2 guides into ISDra2 plant expression vector
pMK025	Cloning vector for PaqCI Golden Gate assembly of ISYmu1 guides into ISYmu1 plant expression vector
pMK024	Cloning vector for PaqCI Golden Gate assembly of ISAam1 guides into ISAam1 plant expression vector
pMK026	ISDra2 g12 cloned into pMK003
pMK027	ISDra2 g13 cloned into pMK003
pMK028	ISDra2 g8 cloned into pMK003
pMK029	ISDra2 g14 cloned into pMK003
pMK030	ISDra2 g4 cloned into pMK003
pMK031	ISDra2 g15 cloned into pMK003
pMK032	ISDra2 g17 cloned into pMK003
pMK033	ISDra2 g18 cloned into pMK003
pMK034	ISDra2 g5 cloned into pMK003
pMK035	ISDra2 g20 cloned into pMK003
pMK036	ISDra2 g22 cloned into pMK003
pMK037	ISDra2 g1 cloned into pMK003
pMK038	ISDra2 g2 cloned into pMK003
pMK039	ISDra2 g3 cloned into pMK003
pMK040	ISDra2 g16 cloned into pMK003
pMK041	ISDra2 g19 cloned into pMK003
pMK042	ISDra2 g9 cloned into pMK003
pMK043	ISDra2 g21 cloned into pMK003
pMK044	ISDra2 g11 cloned into pMK003
pMK045	ISDra2 g7 cloned into pMK003
pMK060	ISYmu1 g1 cloned into pMK025
pMK061	ISYmu1 g2 cloned into pMK025
pMK062	ISYmu1 g3 cloned into pMK025
pMK063	ISYmu1 g4 cloned into pMK025
pMK064	ISYmu1 g5 cloned into pMK025
pMK065	ISYmu1 g7 cloned into pMK025
pMK066	ISYmu1 g8 cloned into pMK025
pMK067	ISYmu1 g9 cloned into pMK025
pMK068	ISYmu1 g10 cloned into pMK025
pMK070	ISYmu1 g12 cloned into pMK025

pMK050	ISAam1 g11 cloned into pMK024
pMK051	ISAam1 g12 cloned into pMK024
pMK052	ISAam1 g13 cloned into pMK024
pMK053	ISAam1 g14 cloned into pMK024
pMK054	ISAam1 g15 cloned into pMK024
pMK055	ISAam1 g16 cloned into pMK024
pMK056	ISAam1 g17 cloned into pMK024
pTW2065	ISYmu1 gRNA2 TRV2 Architecture_A
pTW2066	ISYmu1 gRNA2 TRV2 Architecture_B
pTW2082	ISYmu1 gRNA12 TRV2 Architecture_B

269

Table S4. Oligos used for cloning gRNA sequences into intermediate TnpB plant expression vectors. The Oligo name column is an internal name for each oligo used. The Oligo sequence column lists the sequence of each oligo used for cloning the gRNA. The Oligo description column provides details for cloning each TnpB gRNA target site.

Oligo name	Oligo sequence	Oligo description
MK_29476	TCAAgcgttggagcatataacaga	cloning ISDra2 gRNA_20_bp_gRNA_12_Top
Trevor_28675	GGCCtctgttatatgctccaacgc	cloning ISDra2 gRNA_20_bp_gRNA_12_Bottom
MK_29477	TCAAttacgaattgatgaccatat	cloning ISDra2 gRNA_20_bp_gRNA_1_Top
Trevor_28677	GGCCatatggtcatcaattcgtaa	cloning ISDra2 gRNA_20_bp_gRNA_1_Bottom
MK_29478	TCAAaaggcaaattcgccgcagaa	cloning ISDra2 gRNA_20_bp_gRNA_2_Top
Trevor_28679	GGCCttctgcggcgaatttgcctt	cloning ISDra2 gRNA_20_bp_gRNA_2_Bottom
MK_29479	TCAAtaaagagaggaaattgcagg	cloning ISDra2 gRNA_20_bp_gRNA_13_Top
Trevor_28681	GGCCcctgcaatttcctctcttta	cloning ISDra2 gRNA_20_bp_gRNA_13_Bottom
MK_29480	TCAAtggtctcactttccgaatta	cloning ISDra2 gRNA_20_bp_gRNA_8_Top
Trevor_28683	GGCCtaattcggaaagtgagacca	cloning ISDra2 gRNA_20_bp_gRNA_8_Bottom
MK_29481	TCAAtcacattaagcctagaaact	cloning ISDra2 gRNA_20_bp_gRNA_3_Top
Trevor_28685	GGCCagtttctaggcttaatgtga	cloning ISDra2 gRNA_20_bp_gRNA_3_Bottom
MK_29482	TCAAggtagagctgataagatata	cloning ISDra2 gRNA_20_bp_gRNA_14_Top
Trevor_28687	GGCCtatatcttatcagctctacc	cloning ISDra2 gRNA_20_bp_gRNA_14_Bottom
MK_29483	TCAAcccaagttctccaaataaat	cloning ISDra2 gRNA_20_bp_gRNA_4_Top
Trevor_28689	GGCCatttatttggagaacttggg	cloning ISDra2 gRNA_20_bp_gRNA_4_Bottom
MK_29484	TCAAaaaattggattaatgtgcac	cloning ISDra2 gRNA_20_bp_gRNA_15_Top
Trevor_28691	GGCCgtgcacattaatccaatttt	cloning ISDra2 gRNA_20_bp_gRNA_15_Bottom
MK_29485	TCAAcaatacaaataaatacatgc	cloning ISDra2 gRNA_20_bp_gRNA_17_Top
Trevor_28693	GGCCgcatgtatttatttgtattg	cloning ISDra2 gRNA_20_bp_gRNA_17_Bottom
MK_29486	TCAAcaattcaagctaattataga	cloning ISDra2 gRNA_20_bp_gRNA_18_Top
Trevor_28695	GGCCtctataattagcttgaattg	cloning ISDra2 gRNA_20_bp_gRNA_18_Bottom
MK_29487	TCAAtactattaaatgtcaaaatc	cloning ISDra2 gRNA_20_bp_gRNA_16_Top
Trevor_28697	GGCCgattttgacatttaatagta	cloning ISDra2 gRNA_20_bp_gRNA_16_Bottom
MK_29488	TCAAtacccatcctaaagtatggg	cloning ISDra2 gRNA_20_bp_gRNA_5_Top
Trevor_28699	GGCCcccatactttaggatgggta	cloning ISDra2 gRNA_20_bp_gRNA_5_Bottom
MK_29489	TCAAgagcttaacttggtagagta	cloning ISDra2 gRNA_20_bp_gRNA_19_Top
Trevor_28701	GGCCtactctaccaagttaagctc	cloning ISDra2 gRNA_20_bp_gRNA_19_Bottom
MK_29490	TCAAttgtcagctttcttatggat	cloning ISDra2 gRNA_20_bp_gRNA_20_Top
Trevor_28703	GGCCatccataagaaagctgacaa	cloning ISDra2 gRNA_20_bp_gRNA_20_Bottom
MK_29491	TCAAagctttgaaccggtttcttc	cloning ISDra2 gRNA_20_bp_gRNA_9_Top
Trevor_28705	GGCCgaagaaaccggttcaaagct	cloning ISDra2 gRNA_20_bp_gRNA_9_Bottom
MK_29492	TCAAgttgattaacttgtactacc	cloning ISDra2 gRNA_20_bp_gRNA_21_Top
Trevor_28707	GGCCggtagtacaagttaatcaac	cloning ISDra2 gRNA_20_bp_gRNA_21_Bottom
MK_29493	TCAAtaacttgtactacctcatcc	cloning ISDra2 gRNA_20_bp_gRNA_22_Top
Trevor_28709	GGCCggatgaggtagtacaagtta	cloning ISDra2 gRNA_20_bp_gRNA_22_Bottom
MK_29494	TCAAcgaaaactgaagaacacata	cloning ISDra2 gRNA_20_bp_gRNA_11_Top

Trevor_28711	GGCCtatgtgttcttcagttttcg	cloning ISDra2 gRNA_20_bp_gRNA_11_Bottom
MK_29495	TCAAaaattcaacatctttctcta	cloning ISDra2 gRNA_20_bp_gRNA_7_Top
Trevor_28713	GGCCtagagaaagatgttgaattt	cloning ISDra2 gRNA_20_bp_gRNA_7_Bottom
MK_29758	TCAAttacgaattgatgacc	cloning ISYmu1 gRNA_16_bp_gRNA_1_Top
MK_29759	GGCCggtcatcaattcgtaa	cloning ISYmu1 gRNA_16_bp_gRNA_1_Bottom
MK_29760	TCAAaaggcaaattcgccgc	cloning ISYmu1 gRNA_16_bp_gRNA_2_Top
MK_29761	GGCCgcggcgaatttgcctt	cloning ISYmu1 gRNA_16_bp_gRNA_2_Bottom
MK_29762	TCAAtcacattaagcctaga	cloning ISYmu1 gRNA_16_bp_gRNA_3_Top
MK_29763	GGCCtctaggcttaatgtga	cloning ISYmu1 gRNA_16_bp_gRNA_3_Bottom
MK_29764	TCAAcccaagttctccaaat	cloning ISYmu1 gRNA_16_bp_gRNA_4_Top
MK_29765	GGCCatttggagaacttggg	cloning ISYmu1 gRNA_16_bp_gRNA_4_Bottom
MK_29766	TCAAtacccatcctaaagta	cloning ISYmu1 gRNA_16_bp_gRNA_5_Top
MK_29767	GGCCtactttaggatgggta	cloning ISYmu1 gRNA_16_bp_gRNA_5_Bottom
MK_29770	TCAAaaattcaacatctttc	cloning ISYmu1 gRNA_16_bp_gRNA_7_Top
MK_29771	GGCCgaaagatgttgaattt	cloning ISYmu1 gRNA_16_bp_gRNA_7_Bottom
MK_29772	TCAAtggtctcactttccga	cloning ISYmu1 gRNA_16_bp_gRNA_8_Top
MK_29773	GGCCtcggaaagtgagacca	cloning ISYmu1 gRNA_16_bp_gRNA_8_Bottom
MK_29774	TCAAagctttgaaccggttt	cloning ISYmu1 gRNA_16_bp_gRNA_9_Top
MK_29775	GGCCaaaccggttcaaagct	cloning ISYmu1 gRNA_16_bp_gRNA_9_Bottom
MK_29776	TCAAtaacttgtactacctc	cloning ISYmu1 gRNA_16_bp_gRNA_10_Top
MK_29777	GGCCgaggtagtacaagtta	cloning ISYmu1 gRNA_16_bp_gRNA_10_Bottom
MK_29780	TCAAgcgttggagcatataa	cloning ISYmu1 gRNA_16_bp_gRNA_12_Top
MK_29781	GGCCttatatgctccaacgc	cloning ISYmu1 gRNA_16_bp_gRNA_12_Bottom
MK_29818	TCACcaattcatctggtatc	cloning ISAam1 gRNA_16_bp_gRNA_11_Top
MK_29819	GGCCgataccagatgaattg	cloning ISAam1 gRNA_16_bp_gRNA_11_Bottom
MK_29820	TCACccaagaacaagcctta	cloning ISAam1 gRNA_16_bp_gRNA_12_Top
MK_29821	GGCCtaaggcttgttcttgg	cloning ISAam1 gRNA_16_bp_gRNA_12_Bottom
MK_29822	TCACgttttgtcctcttctc	cloning ISAam1 gRNA_16_bp_gRNA_13_Top
MK_29823	GGCCgagaagaggacaaaac	cloning ISAam1 gRNA_16_bp_gRNA_13_Bottom
MK_29824	TCACcaatttacctatctta	cloning ISAam1 gRNA_16_bp_gRNA_14_Top
MK_29825	GGCCtaagataggtaaattg	cloning ISAam1 gRNA_16_bp_gRNA_14_Bottom
MK_29826	TCACcacataattgaaaaga	cloning ISAam1 gRNA_16_bp_gRNA_15_Top
MK_29827	GGCCtcttttcaattatgtg	cloning ISAam1 gRNA_16_bp_gRNA_15_Bottom
MK_29828	TCACaatttgttacacaact	cloning ISAam1 gRNA_16_bp_gRNA_16_Top
MK_29829	GGCCagttgtgtaacaaatt	cloning ISAam1 gRNA_16_bp_gRNA_16_Bottom
MK_29830	TCACtttgtgtggtatttaa	cloning ISAam1 gRNA_16_bp_gRNA_17_Top

MK_29831	GGCCttaaataccacacaaa	cloning ISAam1 gRNA_16_bp_gRNA_17_Bottom

276 **Table S5. Cloning TRV Cargo Architecture_A and Architecture_B plasmids.** The Plasmid
277 column lists the name of each plasmid created. The PCR template column lists the name of each
278 plasmid used as the DNA template for PCR. The Primer 1 and Primer 2 columns provide the
279 sequence used to amplify fragments using the corresponding PCR template. The reaction column
280 indicates the individual reaction for each PCR. The three PCR reactions, along with the
281 restriction enzyme digested pDK3888 plasmid, were used for NEB HiFi assembly to create the
282 TRV2 vector listed in the Plasmid column.

Plasmid	PCR template	Primer 1	Primer 2	Reaction #
pTW2065	pDK3888	gaatttcctttaccattgacgtcagtgtcgttggtagcat	tgtaatccatCTCGTTAACTCGGGTAAGTGATACA	1
pTW2065	pMK061	AGTTAACGAGatggattacaaggatgatgatgataagga	CCAACTGAGCTACGGgcggcgaatttgccttTTGA	2
pTW2065	pDK3888	aggcaaattcgccgcCCGTAGCTCAGTTGGTTAGAGC	TGGTCACCTGTAATTCACACGTGGTGGTGGTGGTGGT	3
pTW2066	pDK3888	gaatttcctttaccattgacgtcagtgtcgttggtagcat	tgtaatccatCTCGTTAACTCGGGTAAGTGATACA	1
pTW2066	pMK061	AGTTAACGAGatggattacaaggatgatgatgataagga	TCTAACCAACTGAGCTACGGgtcccattcgccatgcc	2
pTW2066	pDK3888	catggcgaatgggacCCGTAGCTCAGTTGGTTAGAGC	TGGTCACCTGTAATTCACACGTGGTGGTGGTGGTGGT	3
pTW2082	pDK3888	gaatttcctttaccattgacgtcagtgtcgttggtagcat	tgtaatccatCTCGTTAACTCGGGTAAGTGATACA	1
pTW2082	pMK070	AGTTAACGAGatggattacaaggatgatgatgataagga	TCTAACCAACTGAGCTACGGgtcccattcgccatgcc	2
pTW2082	pDK3888	catggcgaatgggacCCGTAGCTCAGTTGGTTAGAGC	TGGTCACCTGTAATTCACACGTGGTGGTGGTGGTGGT	3

283

Table S6. Primers used for amp-seq. The TnpB and Guide columns indicate the site being targeted for each TnpB. The F primer and R primer columns list the oligo sequences used to amplify genomic DNA for amp-seq.

TnpB	Guide	F primer	R primer
ISDra2	gRNA1	ACACTCTTTCCCTACACGACGCTCTTCCGATCTaccaaattacgttgagatgcatggtc	GTGACTGGAGTTCAGACGTGTGCTCTTCCGATCTgctcttttgttgcttacgaaacatgt
ISDra2	gRNA2	ACACTCTTTCCCTACACGACGCTCTTCCGATCTgaagcagttgtgagttaagttggaga	GTGACTGGAGTTCAGACGTGTGCTCTTCCGATCTttgtcttaagcgcttgagaagtgg
ISDra2	gRNA3	ACACTCTTTCCCTACACGACGCTCTTCCGATCTatgtcttcagtcttgtgctacacacc	GTGACTGGAGTTCAGACGTGTGCTCTTCCGATCTaaacggaacaaacaagaacctaacct
ISDra2	gRNA4	ACACTCTTTCCCTACACGACGCTCTTCCGATCTtctcttcatgttcttgttggaagtcgg	GTGACTGGAGTTCAGACGTGTGCTCTTCCGATCTgtgctggtaggacatctgggaagt
ISDra2	gRNA5	ACACTCTTTCCCTACACGACGCTCTTCCGATCTgacgtcaggaagaacatggtcatttg	GTGACTGGAGTTCAGACGTGTGCTCTTCCGATCTagaacatttcagcgctaatgctacaa
ISDra2	gRNA7	ACACTCTTTCCCTACACGACGCTCTTCCGATCTtagcttcaaatgagggaccaggctt	GTGACTGGAGTTCAGACGTGTGCTCTTCCGATCTtgtagaggacgacatggttcacagtt
ISDra2	gRNA8	ACACTCTTTCCCTACACGACGCTCTTCCGATCTcacaaacctctgttgcttgaagc	GTGACTGGAGTTCAGACGTGTGCTCTTCCGATCTcattgggtacctaggagctgtaac
ISDra2	gRNA9	ACACTCTTTCCCTACACGACGCTCTTCCGATCTgcgctaaacttataaaccctgatg	GTGACTGGAGTTCAGACGTGTGCTCTTCCGATCTtatgattgccagtgagataaagattc
ISDra2	gRNA11	ACACTCTTTCCCTACACGACGCTCTTCCGATCTgaatcgagattacatgcaggtctta	GTGACTGGAGTTCAGACGTGTGCTCTTCCGATCTccaacactgtatccaactaagtattc
ISDra2	gRNA12	ACACTCTTTCCCTACACGACGCTCTTCCGATCTgaaccgacccgagaagagatttg	GTGACTGGAGTTCAGACGTGTGCTCTTCCGATCTtggaatacacacatttgtacaacca
ISDra2	gRNA13	ACACTCTTTCCCTACACGACGCTCTTCCGATCTtggagttctcgaaatttcatctagtg	GTGACTGGAGTTCAGACGTGTGCTCTTCCGATCTcggaaggatgcagataaactagca
ISDra2	gRNA14	ACACTCTTTCCCTACACGACGCTCTTCCGATCTtctgtaagtccaaaactcataccct	GTGACTGGAGTTCAGACGTGTGCTCTTCCGATCTcttccaacaagaacatgaagagagt
ISDra2	gRNA15	ACACTCTTTCCCTACACGACGCTCTTCCGATCTacagtggttgaactattagttagtgg	GTGACTGGAGTTCAGACGTGTGCTCTTCCGATCTcaaaatctataattagcttgaattgatcaatac
ISDra2	gRNA16	ACACTCTTTCCCTACACGACGCTCTTCCGATCTgtgaggttagtaactatgatgcatgt	GTGACTGGAGTTCAGACGTGTGCTCTTCCGATCTaagacaaatgaccatgttcttcctg
ISDra2	gRNA17	GTGACTGGAGTTCAGACGTGTGCTCTTCCGATCTacagtggttgaactattagttagtgg	ACACTCTTTCCCTACACGACGCTCTTCCGATCTcctcaaacattcatcagttctttgat
ISDra2	gRNA18	GTGACTGGAGTTCAGACGTGTGCTCTTCCGATCTacagtggttgaactattagttagtgg	ACACTCTTTCCCTACACGACGCTCTTCCGATCTcctcaaacattcatcagttctttgat
ISDra2	gRNA19	ACACTCTTTCCCTACACGACGCTCTTCCGATCTaagtaggctattgagttcacagttt	GTGACTGGAGTTCAGACGTGTGCTCTTCCGATCTatgaaaccacaacaccacatg
ISDra2	gRNA20	ACACTCTTTCCCTACACGACGCTCTTCCGATCTcttggtagagtagttagcatgctga	GTGACTGGAGTTCAGACGTGTGCTCTTCCGATCTccctggacaagtatacaattaatcag
ISDra2	gRNA21	ACACTCTTTCCCTACACGACGCTCTTCCGATCTtgttgcagcttatgacacacaataag	GTGACTGGAGTTCAGACGTGTGCTCTTCCGATCTaatctttatctcactggcaatcatag
ISDra2	gRNA22	ACACTCTTTCCCTACACGACGCTCTTCCGATCTtgttgcagcttatgacacacaataag	GTGACTGGAGTTCAGACGTGTGCTCTTCCGATCTaatctttatctcactggcaatcatag
ISYmu1	gRNA1	ACACTCTTTCCCTACACGACGCTCTTCCGATCTaccaaattacgttgagatgcatggtc	GTGACTGGAGTTCAGACGTGTGCTCTTCCGATCTgctcttttgttgcttacgaaacatgt
ISYmu1	gRNA2	ACACTCTTTCCCTACACGACGCTCTTCCGATCTgaagcagttgtgagttaagttggaga	GTGACTGGAGTTCAGACGTGTGCTCTTCCGATCTttgtcttaagcgcttgagaagtgg
ISYmu1	gRNA3	ACACTCTTTCCCTACACGACGCTCTTCCGATCTatgtcttcagtcttgtgctacacacc	GTGACTGGAGTTCAGACGTGTGCTCTTCCGATCTaaacggaacaaacaagaacctaacct
ISYmu1	gRNA4	ACACTCTTTCCCTACACGACGCTCTTCCGATCTtctcttcatgttcttgttggaagtcgg	GTGACTGGAGTTCAGACGTGTGCTCTTCCGATCTgtgctggtaggacatctgggaagt
ISYmu1	gRNA5	ACACTCTTTCCCTACACGACGCTCTTCCGATCTgacgtcaggaagaacatggtcatttg	GTGACTGGAGTTCAGACGTGTGCTCTTCCGATCTagaacatttcagcgctaatgctacaa
ISYmu1	gRNA7	ACACTCTTTCCCTACACGACGCTCTTCCGATCTtagcttcaaatgagggaccaggctt	GTGACTGGAGTTCAGACGTGTGCTCTTCCGATCTaagtacttctgtttgtgtaatctcc
ISYmu1	gRNA8	ACACTCTTTCCCTACACGACGCTCTTCCGATCTcacaaacctctgttgcttgaagc	GTGACTGGAGTTCAGACGTGTGCTCTTCCGATCTcattgggtacctaggagctgtaac
ISYmu1	gRNA9	ACACTCTTTCCCTACACGACGCTCTTCCGATCTgcgctaaacttataaaccctgatg	GTGACTGGAGTTCAGACGTGTGCTCTTCCGATCTtatgattgccagtgagataaagattc
ISYmu1	gRNA10	GTGACTGGAGTTCAGACGTGTGCTCTTCCGATCTgaatctttatctcactggcaatcata	ACACTCTTTCCCTACACGACGCTCTTCCGATCTtgttgcagcttatgacacacaataag

ISYmu1	gRNA12	ACACTCTTTCCCTACACGACGCTCTTCCGATCTgaaccgacccgagaagagatttg	GTGACTGGAGTTCAGACGTGTGCTCTTCCGATCTtggaatacacacatttgtacaacca
ISAam1	gRNA11	GTGACTGGAGTTCAGACGTGTGCTCTTCCGATCTagtttcttactcactaatggaagcac	ACACTCTTTCCCTACACGACGCTCTTCCGATCTaaggagcttcaggatatcgactacaa
ISAam1	gRNA12	GTGACTGGAGTTCAGACGTGTGCTCTTCCGATCTgcaggtgaatttcttatttatgcagt	ACACTCTTTCCCTACACGACGCTCTTCCGATCTgaaggttacttctgcaaaaaacaaca
ISAam1	gRNA13	ACACTCTTTCCCTACACGACGCTCTTCCGATCTcgtctggaccaagaaagttgt	GTGACTGGAGTTCAGACGTGTGCTCTTCCGATCTcagaaacgtgagatgtcaaatctgt
ISAam1	gRNA14	ACACTCTTTCCCTACACGACGCTCTTCCGATCTtgttaagttgttattgtgttctctgg	GTGACTGGAGTTCAGACGTGTGCTCTTCCGATCTgaaaatatgtaaaccagtctcatacc
ISAam1	gRNA15	GTGACTGGAGTTCAGACGTGTGCTCTTCCGATCTcgctgcgtctcctgtttctctac	ACACTCTTTCCCTACACGACGCTCTTCCGATCTccggtggaagcaaatcagac
ISAam1	gRNA16	ACACTCTTTCCCTACACGACGCTCTTCCGATCTtgcaaggaggaggagtatttgg	GTGACTGGAGTTCAGACGTGTGCTCTTCCGATCTtatccgattccgcttagtttgc
ISAam1	gRNA17	GTGACTGGAGTTCAGACGTGTGCTCTTCCGATCTaccaaattacgttgagatgcatggtc	ACACTCTTTCCCTACACGACGCTCTTCCGATCTtggtcttgtttggttttcagacc

287

288 **Table S7. Oligos for RT-PCR.** The name of each oligo is listed in the Oligo name column. Each
289 oligo sequence is provided in the Oligo sequence column, with a description of what the oligos
290 were used for in the Description column.

oligo name	Oligo sequence	Description
SP9238	TGTATAGACTGTTTGAGATCGGCG	RT-PCR primer to check for the presence/absence of TRV in mutant albino plants
SP9239	GTAATAACGCTTACGTAGGCGAGG	RT-PCR primer to check for the presence/absence of TRV in mutant albino plants
IPP2 RT-PCR Fw	GTATGAGTTGCTTCTCCAGCAAAG	RNA control for RT-PCR
IPP2 RT-PCR Rev	GAGGATGGCTGCAACAAGTGT	RNA control for RT-PCR

291